CrossMark

Conditioned Medium from Adipose-Derived Stem Cells (ADSCs) Promotes Epithelial-to-Mesenchymal-Like Transition (EMT-Like) in Glioma Cells In vitro

Isabele C. Iser[1] · Stefanie M. Ceschini[1] · Giovana R. Onzi[2] · Ana Paula S. Bertoni[1] · Guido Lenz[2] · Márcia R. Wink[1]

Abstract Mesenchymal stem cells (MSCs) have recently been described to home to brain tumors and to integrate into the tumor-associated stroma. Understanding the communication between cancer cells and MSCs has become fundamental to determine whether MSC-tumor interactions should be exploited as a vehicle for therapeutic agents or considered a target for intervention. Therefore, we investigated whether conditioned medium from adipose-derived stem cells (ADSCs-CM) modulate glioma tumor cells by analyzing several cell biology processes in vitro. C6 rat glioma cells were treated with ADSCs-CM, and cell proliferation, cell cycle, cell viability, cell morphology, adhesion, migration, and expression of epithelial-mesenchymal transition (EMT)-related surface markers were analyzed. ADSCs-CM did not alter cell viability, cell cycle, and growth rate of C6 glioma cells but increased their migratory capacity. Moreover, C6 cells treated with ADSC-CM showed reduced adhesion and underwent changes in cell morphology. Up-regulation of EMT-associated markers (vimentin, MMP2, and NRAS) was also observed following treatment with ADSC-CM. Our findings demonstrate that the paracrine factors released by ADSCs are able to modulate glioma cell biology. Therefore, ADSC-tumor cell interactions in a tumor microenvironment must be considered in the design of clinical application of stem cell therapy.

Keywords Adipose-derived stem cell · Conditioned medium · C6 glioma cell · Epithelial-mesenchymal transition

✉ Márcia R. Wink
  mwink@ufcspa.edu.br; marciawink@yahoo.com.br

1 Departamento de Ciências Básicas da Saúde e Laboratório de Biologia Celular, Universidade Federal de Ciências da Saúde de Porto Alegre - UFCSPA, Rua Sarmento Leite, 245, CEP 90050-170 Porto Alegre, RS, Brazil

2 Departamento de Biofísica e Centro de Biotecnologia, Universidade Federal do Rio Grande do Sul - UFRGS, Porto Alegre, RS, Brazil

Introduction

Gliomas are the most frequent primary tumors that affect the human brain. Glioblastoma (GBM) is the most common malignant form of glioma and is one of the most aggressive and lethal human cancer. The current survival rate for patients with GBM is about 1 year [1, 2], and this has not changed significantly over the last decade. GBMs are characterized by widespread invasion throughout the brain, marked heterogeneity in appearance and gene expression, and resistance to traditional and newer targeted therapeutic approaches. Despite the available treatments with surgical resection of the tumor, radiotherapy, chemotherapy, and drugs, such as temozolomide, these treatments have shown only slight effects on survival of patients and GBM remains fatal [2–4].

It is now understood that maintaining the mutual and interdependent interaction between tumor and its microenvironment is crucial to orchestrate the fate of tumor progression [5]. A tumor microenvironment is composed of a complex crosstalk of different cell types such as fibroblast, endothelial cells, mesenchymal stem cell (MSCs), and inflammatory cells as well as cytokines and growth factors secreted by these cells [5]. Inflammation is always associated with tumor development where the tissue suffers from chronic injury. Thereby, malignancy may also be considered as a nidus of chronic inflammation or "wound that never heals" [6]. Based on the property of MSCs to be recruited to injured tissues, MSCs can

be attracted to the surrounding tumor stroma and play a role in modulating cancer progression [7].

MSCs are being broadly studied and have emerged as a great promise of the current therapeutic research. The enthusiasm about these cells is mainly due to their ability to differentiate in many cell types, capacity of self-renew, and paracrine activity that includes immunomodulatory effects [8]. Contrary to what was initially thought, the ability to differentiate is not the main feature that makes these cells attractive for therapeutic purposes. There are increasing evidences that the secretions of these cells, such as nucleotides, growth factors, cytokines, and chemokines constitute their most significant therapeutic mechanism of action [9–11]. The tumor homing ability has encouraged researchers to analyze MSCs as a tool in gene therapy, since these cells can act as gene delivery vehicles for anticancer agents [12–15]. However, evidence suggests that interactions between MSCs and cancer cells may impact upon the phenotype of the tumor cells [16–20]. Conflicting reports exist with relation to the effect of MSCs on glioma cells growth, with some studies reporting cytotoxicity against malignant glioma cells [20–23] and others suggesting a pro-tumoral effect [24–28].

Epithelial to mesenchymal transition (EMT) is a process in which cells gradually substitute their epithelial characteristics with a mesenchymal phenotype, that is associated with increased invasion and metastasis [29]. This status is characterized by increased motility, invasiveness, and elevated synthesis of extracellular matrix-degrading enzymes able to degrade the basement membrane, besides loss of cell-cell contact, reorganization of cytoskeletal proteins, and elevated resistance to apoptosis [30, 31]. Notably, the composition of the tumor microenvironment, such as growth factors and cytokines, has recently been suggested to modulate the EMT process in cancer cells [29, 32–35].

In our study, conditioned medium from adipose-derived stem cells (ADSC-CM) from rat did not change the viability, proliferation, or cell cycle distribution of glioma. However, ADSC-CM induced an epithelial-to-mesenchymal-like transition phenotype in tumor cells with increased tumor cell migration, reduced cell adhesion capacity, changed cell morphology, as well as increased expression of mesenchymal-related genes.

Thus, we propose that to ensure the safety of anticancer therapy using MSCs, the characteristics of MSCs themselves, as well as the interaction between stem cells and cancer cells, are quite important and should be investigated before using an MSC-based therapy.

Materials and Methods

Ethical Aspects

The protocols used in this study were approved by the Ethics Committee on Animal Use (CEUA) of Universidade Federal de Ciências da Saúde de Porto Alegre (UFCSPA), under the number 104/11, following the resolutions of the Conselho Nacional de Controle de Experimentação Animal (CONCEA). The NIH "Guide for the Care and Use of Laboratory Animals" (NIH publication N° 80–23, revised 1996) was followed in all experiments. The surgery of ADSC isolation was performed with all efforts to minimize the animal suffering.

Cell Culture

The C6 rat glioma cell line from ATCC was kindly provided by Dra. Ana Maria Oliveira Battastini (UFRGS, Brazil). Cells at 5–20 passages were grown in culture flasks and maintained in Dulbecco's modified Eagle's medium (DMEM) (pH 7.4) containing 1 % DMEM (Sigma, St. Louis, MO, USA), 8.4 mM HEPES, 23.8 mM $NaHCO_3$, 0.1 % amphotericin B, and penicillin (100 U/mL)/streptomycin (100 mg/mL) (Gibco BRL, Grand Island, NY, USA) and supplemented with 10 % (v/v) fetal bovine serum (FBS) (Cultilab, São Paulo, SP, Brazil). Cells were kept at 37 °C, a minimum relative humidity of 95 %, and an atmosphere of 5 % CO_2 in air.

Isolation and Culture of Adipose-Derived Stem Cells

Adipose-derived stem cells (ADSCs) were extracted from visceral adipose tissue of *Wistar* rats (6–8 weeks), as previously described [36]. Briefly, the abdominal fat tissue from rat was transferred to a petri dish, washed with phosphate-buffered saline (PBS), and dissociated mechanically with a pipette. The fat fragments were transferred to a falcon tube containing 2 mg/mL of collagenase type I, solubilized in DMEM medium without FBS, and incubated in a water bath at 37 °C for 30–45 min. After collagenase digestion, the supernatant was transferred to a new tube and centrifuged at 1000 rpm for 10 min at room temperature (RT). The supernatant was discarded, and cells were resuspended in complete medium and seeded in six-well dishes. ADSC cultures were grown in culture flasks and maintained in DMEM low glucose, containing 8.4 mM HEPES (pH 7.4), 23.8 mM $NaHCO_3$, 0.1 % amphotericin B, and penicillin (100 U/mL)/streptomycin (100 mg/mL) (Gibco BRL, Grand Island, NY, USA) and supplemented with 10 % (v/v) FBS (Cultilab, São Paulo, SP, Brazil). Cells were kept at a temperature of 37 °C and humidity of 95 %/5 % CO_2 in air.

ADSC Differentiation

Osteogenic differentiation was induced by culturing ADSCs up to 8 weeks in Differentiation SingleQuots™ (Lonza, Walkersville, MD, USA) plus 5 µg/mL of ascorbic acid. In order to observe calcium deposition, cultures were washed once with PBS, fixed with 4 % paraformaldehyde in PBS for 15–30 min, and stained for 5 min at RT with alizarin red S stain

at pH 4.2. Excess of stain was removed by several washes with distilled water. To induce adipogenic differentiation, ADSCs were cultured up to 8 weeks in DMEM supplemented with 10^{-8} M dexamethasone, 2.5 mg/mL insulin, and 100 mM indomethacin. To further confirm their identity, cells were fixed with 4 % paraformaldehyde in PBS for 1 h at RT and stained with oil red O solution. Chondrogenic differentiation was performed using differentiation CDMTM basal medium and CDMTM Differentiation SingleQuots™ (Lonza). Cultures were analyzed by fixing with 4 % paraformaldehyde in PBS for 20 min and staining with alcian blue (pH 2.5) (Sigma, St. Louis, MO, USA) in 3 % acetic acid for 5 min at RT. After staining, the cultures were washed with distilled water.

Immunophenotyping

The cultures of ADSCs were characterized to confirm the presence or absence of MSC surface markers using flow cytometry. Cells were trypsinized, centrifuged, and incubated for 25 min at 4 °C with phycoerythrin (PE)- or peridinin-chlorophyll protein (PerCP-Cy5.5)-conjugated antibodies with anti-rat CD45, CD29, or CD90.2 (Life Technologies, Carlsbad, CA, USA). The unconjugated antibody CD11b (Life Technologies, Carlsbad, CA, USA) was incubated with the secondary anti-mouse IgG2 FITC-conjugated antibody (Sigma-Aldrich, St. Louis, MO, USA) for an additional 25 min. Excess of antibody was removed by washing with PBS (phosphate-buffered saline). Cells were analyzed using a FACSCalibur cytometer equipped with a 488-nm argon laser (Becton Dickinson, San Diego, CA, USA) with the CellQuest software. At least 10,000 events were collected. Gating was set using unstained cells.

Conditioned Medium

For all experiments, ADSC cells between the fourth and tenth passages were seeded in T75 tissue culture flask in DMEM with 10 % (*v/v*) FBS low glucose, containing 8.4 mM HEPES (pH 7.4), 23.8 mM NaHCO$_3$, 0.1 % amphotericin B, and penicillin (100 U/mL)/streptomycin (100 mg/mL) (Gibco BRL, Grand Island, NY, USA) at a density of 3320 cells/cm^2. Twenty-four hours after seeding, the medium was replaced by a fresh medium and conditioned for 24 h (CM24) or 48 h (CM48). CM from flasks was harvested, filtrated on 0.22 μm filters (Millipore), and stored at −80 °C until use.

Assessment of Glioma Cell Viability

C6 cells were seeding with 3 mL of DMEM/10 % FBS without phenol red in each flask of 25 cm^2 (in triplicate) and allowed to grow until reaching a 70 % confluence. After, C6 cells were exposed to CM24 and CM48 (prepared using DMEM without phenol red to avoid color interference) during

24 and 48 h. After this time, aliquots of culture medium were taken out for viability analysis. Cell integrity was assessed by measuring the release of the cytosolic enzyme lactate dehydrogenase (LDH) into the medium. LDH activity was detected by automatic biochemical analyzer (Mindray BS-120, Shenzhen, GNG, China) with the commercial bio-kit (Bioclin, Belo Horizonte, Brazil) at 340 nm according to the manufacturer's protocol. Supernatants of cells treated for 24 and 48 h with DMEM without phenol red was used as negative control. Positive control was performed after cell lysis by addition of 1 % Triton X-100. Results were expressed as the percentage of LDH release against the positive control.

Cell Cycle Analysis

In order to evaluate a possible interference of CM in cell cycle progression, we adapted the protocol of the method described by Overton and McCoy [37]. Cells were plated in six-well plates (5×10^4 cell/well) for 1 day, and after they were treated with CM24 and CM48 for 24 and 48 h, respectively. Cells were trypsinized, centrifuged, and washed with PBS twice. Then, cells were resuspended in ice-cold ethanol 70 % (*v/v* in PBS) and left for 24 h at 4 °C. On the next day, fixed cells were washed with PBS and marked with a solution containing 0.3 mg/mL RNAse, 20 μg/mL propidium iodide, and 0.1 % Triton X-100 for 30 min, in the dark, at RT. Marked cells were analyzed in a FACSCalibur flow cytometer (BD Pharmingen) using the CellQuest program suite to evaluate DNA content of cells and thus cell cycle distribution of samples. Approximately 10,000 cells were analyzed in each experiment. All analyses were performed at least three times.

Proliferation Assays

The ability of CM24 and CM48 to induce cellular proliferation was evaluated by using MTT 3-(4,5 dimethylthiazol-2-thiazyl)-2,5-diphenyl-tetrazolium bromide assay (MTT, Sigma-Aldrich, St. Louis, MO, USA). Briefly, C6 cells (2×10^3 cell/well) were seeded in 96-well plates. After 24 h, cells were washed and treated with CM. After 24 or 48 h, MTT solution (5 mg/mL) was added and cells were incubated at 37 °C for 3 h. The supernatant was aspirated, and the formazan crystals were solubilized in dimethyl sulfoxide (DMSO; 100 μL). The absorbance, proportional to the number of viable cells, was measured at 570 nm by a multiwell spectrophotometer (SpectraMax Plus Microplate Spectrophotometer, Molecular Devices, US). Results were expressed as the absolute values of results from replicate wells.

To evaluate the proliferation rate in a long-term culture of C6 cells in response to treatment with CM24 and CM48, cumulative population doublings were determined in the PD assay. Cells were plated in 24-well plates at a concentration of 1.5×10^4 cells/well and exposed to CM during 24 or 48 h.

Confluent cells were passaged, and population doublings (PD) were determined according to the formula PD = [log N(t) − log N(to)]/log 2, where N(t) is the number of cells per well at time of passage, and N(to) is the number of cells seeded at the previous passage. The sum of PDs was then plotted against time of culture. Cells were followed until day 20.

Adhesion Assay

C6 cells were treated with CM24 or CM48 for 24 and 48 h, respectively. Then, cells were seeded at density of 3×10^4 cells/well in 96-well plates and incubated with CM24 and CM48 for 1 h at 37 °C with a 5 % CO_2 enriched atmosphere. The non-adherent cells were removed by washing carefully three times with PBS. Adherent cells were fixed with 4 % paraformaldehyde (PFA) for 10 min and stained for 10 min with 100 μL 0.5 % crystal violet diluted in 20 % methanol. The cells were then washed three times with Milli-Q^{TM} water, and the stain was eluted in 100 μL 10 % acetic acid (v/v). Cell adhesion was analyzed by measuring optical density (OD) at 570 nm in a microplate reader [38].

Migration Assays

Scratch Wound Healing

C6 cells were plated in 24-well culture plates and grown in complete medium until reaching 80 % of confluence. Then, monolayers were scratched using a 200 μL sterile plastic pipette tip as previously described [39] and washed three times with PBS. After, cells were treated with CM24 and CM48 serum free (SF) during 24 h. Positive controls were performed with DMEM+ 10 % FBS and negative controls with DMEM SF. Scratch wound closure was monitored by phase microscopy using a ×4 objective at 0, 4, 8, 12, and 24 h.

Transwell Assay

In parallel, cell migration was also evaluated using a 24-well Transwell chamber (Greiner, Frickenhausen, Germany). For this purpose, 2.5×10^4 C6 cells were seeded in the upper chamber of a 8-μm pore size insert and allowed to migrate toward a DMEM + 10 % FBS (positive control) or DMEM without FBS (negative control) or ADSC (1.4×10^4 cells/well) present in the lower chamber. Cells were incubated for 24 and 48 h, then the non-migrating cells of the upper chamber were removed with the aid of a cotton swab and the remaining cells were fixed in methanol. Cells that migrated to the lower surface of the membrane were stained with 0.5 % crystal violet diluted in 20 % methanol and counted with a microscope (Olympus BX-50 coupled to a Moticam 2500 camera). Four visual fields were randomly chosen for each assay. The quantitation was performed by processing all obtained images using Image J software (http://imagej.nih.gov/ij/). The average number of the migrating cells in these four fields was taken as the cell migration number of the group [40].

Actin Cytoskeleton Staining

Actin cytoskeleton reorganization was assessed via filamentous actin (F-actin) staining, as reported previously [41]. Briefly, cultured C6 cells seeded on glass coverslips were treated with CM24, CM48, or TGFβ (1 μg/L) during 24 h, 48 h, and 5 days. After each treatment, cells were washed with PBS and fixed with 4 % paraformaldehyde for 24 h. Then, cells were stained with phalloidin-fluorescein isothiocyanate and the nucleus was stained with 4′,6-diamidino-2-phenylindole dihydrochloride (DAPI; 300 nM; Sigma) for 30 min. Images of the fluorescently labeled stress fibers were captured using an Olympus BX-50 with optical lens (×10/0.30 Ph1-UplanFI) coupled to a Moticam 2500 camera.

Nuclear Morphometric Analysis (NMA)

Nuclear morphometry was analyzed as described by Filippi-Chiela [42]. Briefly, cells were treated with ADSC-CM or TGFβ (24 h, 48 h, and 5 days), fixed with 4 % paraformaldehyde (v/v in PBS) for 30 min at room temperature, and stained with DAPI 300 nM for 30 min, followed by quantification of DAPI-stained nuclei using the Software Image Pro Plus 6.0 (Media Cybernetics, Silver Spring, MD). Images of the DAPI-labeled nuclei were captured using an Olympus BX-50 with

Table 1 Primers for EMT markers used at RT-qPCR experiments

Primer	Sense	Antisense
MMP2	5′-ACAACAGCTGTACCACCGAG-3′	5′-GGACATAGCAGTCTCTGGGC-3′
Vimentin	5′-GAGGAGATGAGGGGAGTTGCG-3′	5′-GGTCAAGACGTGCCAGAGAA-3′
NRAS	5′-CACGAGCTGGCCAAGAGTTA-3′	5′-TGAGGCTTGAAAGTGGCTCG-3′
Src	5′-CTTCCTCTCACTAGGCCTGC-3′	5′-CTTCCTCTCACTAGGCCTGC-3′
TBP	5′-CGTGACGATAACCCAGAAAG-3′	5′-GGTGGAAGGCTGTTGTTC-3′

EMT epithelial-mesenchymal transition, *MMP2* matrix metalloproteinase-2, *Src* proto-oncogene tyrosine-protein kinase, *RT-qPCR* quantitative reverse transcription-polymerase chain reaction

optical lens (×10/0.30 Ph1-UplanFl) coupled to a Moticam 2500 camera. Data are presented as a plot of area versus nuclear irregularity index (NII).

RT-qPCR Analysis

Total RNA from glioma cell cultures were isolated with TRIzol LS reagent (Life Technologies, Carlsbad, CA, USA) in accordance with the manufacturer's instructions and stored at −80 °C.

The complementary DNA (cDNA) was synthesized with M-MLV reverse transcriptase enzyme (Promega, Madison, WI, USA) 3 µg total RNA in a final volume of 20 µL with a random hexamer primer in accordance with the manufacturer's instructions. cDNA was diluted to 1:10 in diethyl pyrocarbonate (DEPC) water and stored at −20 °C. Real-time PCRs were carried out in an Applied Biosystems StepOnePlus™ Real-Time PCR cycler and done in duplicate.

Reaction settings were composed of an initial enzyme activation step of 20 s at 95 °C, followed by 40 cycles of 3 s at 95 °C and 30 s at 60 °C for data acquisition. Real-time PCRs were prepared in a 12.5-µL final volume composed of 6.25 µL of Fast SYBR green master mix (Applied Biosystems, Foster City, CA, USA), 0.40 µL of 10 µM primer pairs (Table 1), 3.85 µL of water, and 2 µL of diluted cDNA. After an appropriate selection using relative standard curve method, TBP was chosen as the most stable reference gene between five gene candidates and was used as a control for cDNA synthesis [43]. All results were analyzed by the $2^{-\Delta\Delta CT}$ method [44]. The data were presented as ratio of genes/TBP.

Statistics

All data were expressed as mean ± SEM, and they were analyzed using t test for single comparisons or ANOVA followed
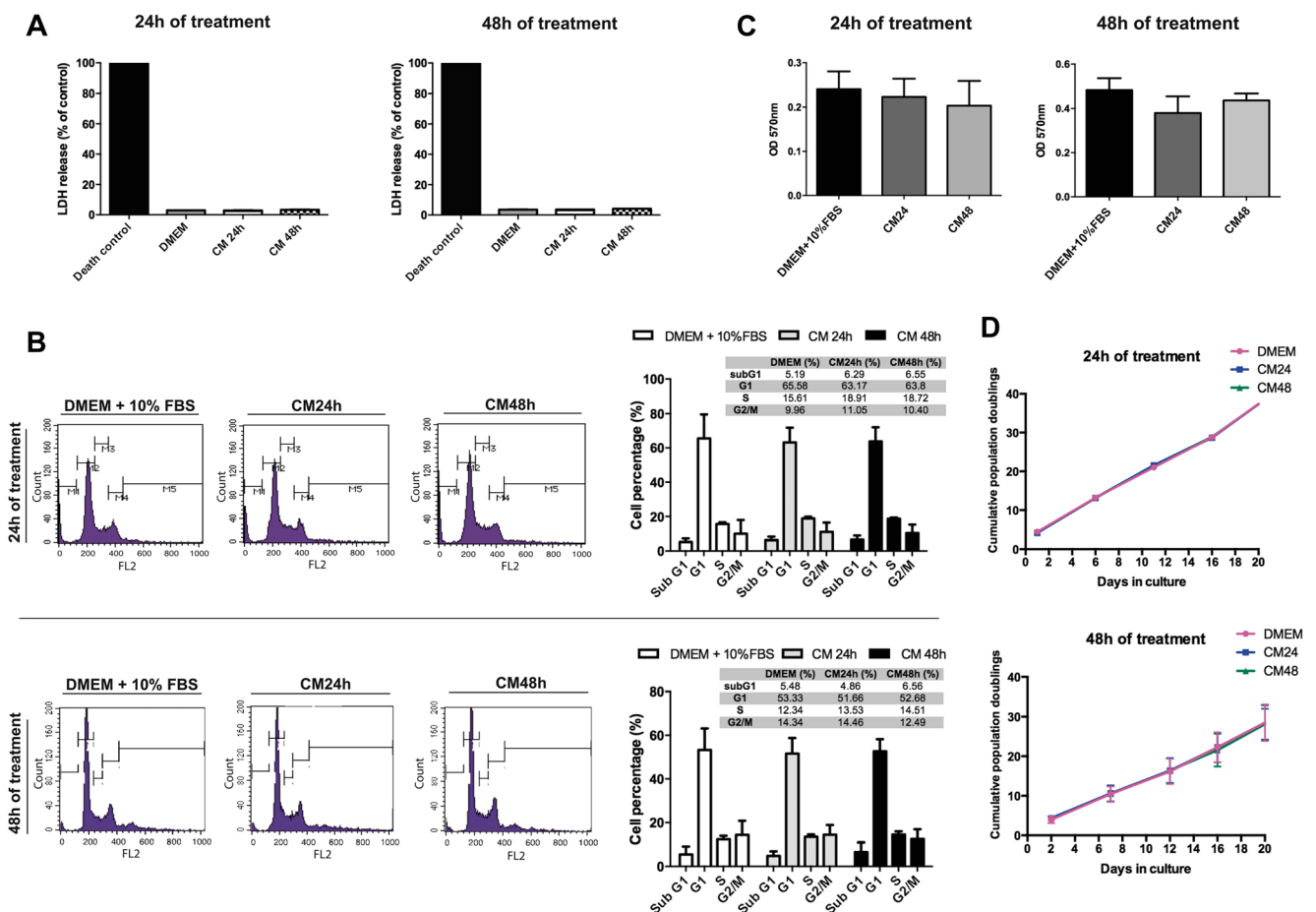

Fig. 1 Effect of ADSC-CM on LDH release, cell cycle distribution, and cell proliferation rate in C6 glioma cells. **a** The cytotoxicity of ADSC-CM was evaluated by measuring the LDH enzymatic activity on supernatant of C6 cells treated with ADSC-CM for 24 and 48 h. **b** Flow cytometry was used for determination of cell cycle distribution (sub-G1, G1/G0, S, and G2/M) in untreated and ADSC-CM-treated (24 and 48 h) C6 cells. **c** Cell cultures were exposed to ADSC-CM for 24 and 48 h, and cell proliferation was assessed by the MTT assay as described in the

"Materials and Methods" section. Glioma cultures treated with 10 % FBS was taken as 100 % of cell proliferation. **d** C6 cells were cultivated in the presence of ADSC-CM for 24 and 48 h, and cumulative population doublings were plotted against time. Results are expressed in percentage and were analyzed by one-way ANOVA, followed by Tukey's multiple comparisons test. The values were considered significantly different from controls, when $P < 0.05$. All experiments were repeated at least three times
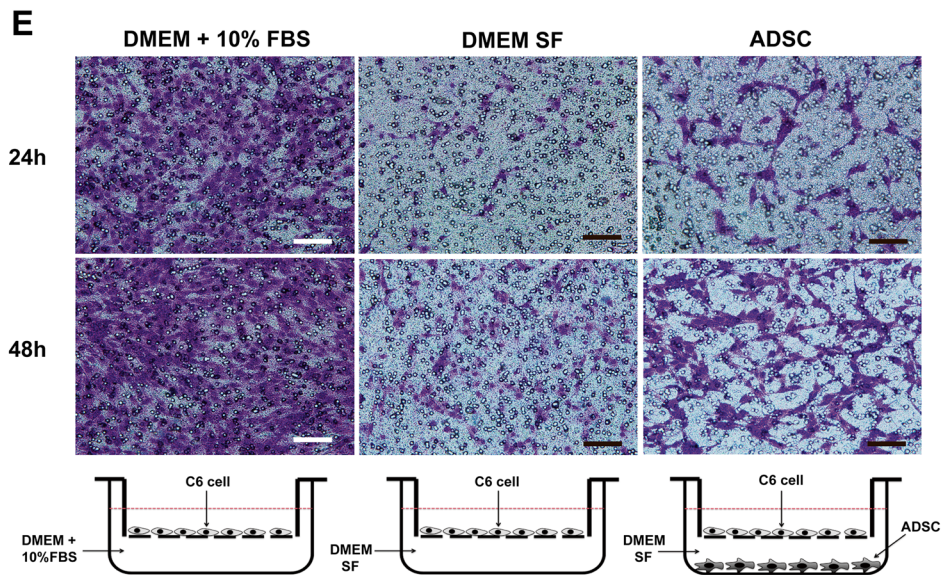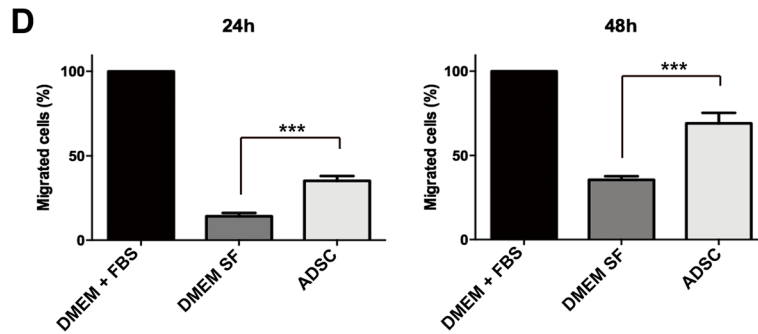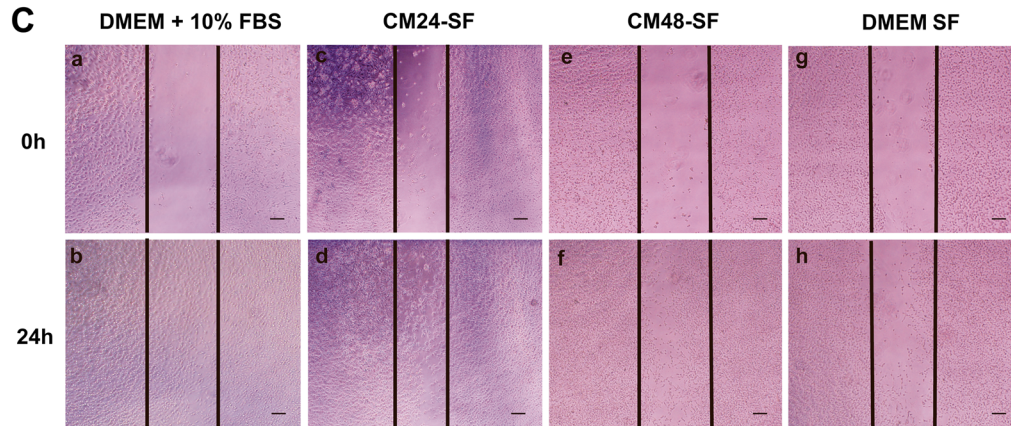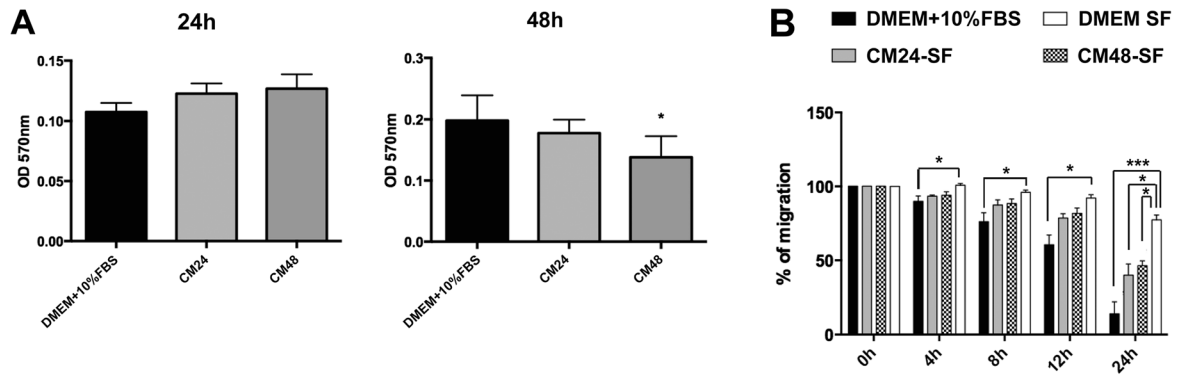
◀ **Fig. 2** Effect of ADSC-CM on glioma cell adhesion and migration. **a** Semi-confluent cultures of C6 cells were treated with ADSC-CM for 1 h. Then, cell adhesion was evaluated as described in the "Materials and Methods" section. **b** C6 cells wound repair after 24 h with ADSC-CM-SF. Negative controls indicates wound repair with DMEM SF. Positive control represent wound repair with 10 % FBS supplemented DMEM. The average initial wound width was measured and defined as 100 %. **c** Inverted light microscopic images of C6 cells wound repair. Negative and positive controls indicate DMEM SF and complete DMEM + 10 % FBS, respectively. Wound healing within the scrape line was recorded every day. Representative scrape lines are shown at 0 and 24 h; *dashed line* indicated the margin of the scratch. *Scale bars* 200 μm. **d** ADSC-CM affected cell migration by Transwell assay. C6 cell seeded in the upper chamber of Transwells were incubated with ADSC added to the lower chamber, and cell migration was determined during 24 and 48 h, as described in the "Materials and Methods" section. DMEM + 10 % FBS and DMEM SF were used as the positive and negative control, respectively. Cells were photographed, and average cells per field were calculated. *Columns* represent the mean percentage of migrating cells relative to the negative control. **e** Representative light microscopy image of crystal violet stained cells on the basal surface of the filter and scheme illustrating each assay. *Scale bars* 100 μm. *p < 0.05 and ***p < 0.001 indicate significant differences in relation to the control group as determined by ANOVA followed by Tukey's test. All experiments were repeated at least three times

by Tukey's test for multiple comparisons of at least three independent experiments. Differences with *p* < 0.05 were considered significant. Analysis of the data was performed using GraphPad Prism version 6.0 software (Graphpad, La Jolla, CA, USA).

Results

ADSCs Express Stem Cell Markers and Display Multipotent Differentiation

The ADSCs population was characterized by the CD marker profile using flow cytometry analysis. As already reported [45], ADSCs expressed CD90 (glycosylphosphatidylinositol-anchored glycoprotein) and CD29 (integrin b1 chain), whereas CD11b and CD45, hematopoietic surface markers, were negative (Supplementary Fig. 1A). In our study, ADSCs isolated from visceral adipose tissue presented the expected elongated fusiform morphology and capacity to differentiate into osteogenic, adipogenic, or chondrogenic lineages (Supplementary Fig. 1B, C and D).

ADSC-CM Neither Damages the Cell Membrane of C6 Cells Nor Induces Cell Cycle Arrest and Changes in Growth Rate of C6 Glioma Cells

First, we examined if the ADSC-CM could affect the viability of glioma C6 by treating cells with CM24 and CM48 for 24 and 48 h, respectively. At the end of incubation, LDH activity was determined in supernatants. This assay showed that

ADSC-CM did not cause a significant release of LDH into culture medium of C6 cells, indicating that the factors present in CM are unable to generate loss in cell membrane integrity (Fig. 1a).

To explore the influence of ADSC-CM on cell cycle progression, the proportion of cells in the G1, S, and G2/M phases was determined in the presence or absence of CM24 and CM48 after 24 and 48 h of treatment, respectively. The flow cytometry analyses using PI for DNA labeling showed that both CM24 and CM48 were unable to change the relative content of cells in the cell cycle phases (Fig. 1b).

In order to determine the proliferation rate of C6 glioma, cell cultures were treated with CM24 and CM48 and MTT assay was performed (Fig. 1c). Exposure of glioma cells to CM for 24 and 48 h did not result in alteration of cell proliferation. After 24 or 48 h of treatment, the absorbance of cells treated with CM24 and CM48 was not statistical different from control cells.

Finally, to investigate the influence of ADSC-CM on a long-time proliferation rate, the PD was performed. After the treatment with ADSC-CM during 24 and 48 h, glioma cells were followed for 20 days. Our results showed that ADSC-CM does not affect the PD rate of C6 cells, suggesting that the factors contained in CM do not lead to a significant change in cell growth and cell senescence (Fig. 1d).

ADSC-CM-Pretreated Tumor Cells are Able to Induce EMT-Like Plasticity

ADSC-CM Decreases C6 Cell Adhesion

Epithelial-mesenchymal transition (EMT) is a recognized process often associated to development and cancer progression [46]. Enhanced invasive capacity with loss of intercellular adhesion proteins and acquisition of the more motile mesenchymal phenotype are among the characteristics of EMT [47]. Considering the importance of this process in tumorigenesis, we investigate if ADSC-CM-treated tumor cells could undergo an EMT-like process. To this end, we evaluated several parameters, starting by performing cell adhesion assay.

The results showed that ADSC-CM24 and ADSC-CM48 are unable to change glioma cell adhesion during 24 h of treatment. On the other hand, after 48 h of treatment, ADSC-CM48 promoted a decrease of 20 % in glioma cell adhesion (Fig. 2a).

ADSC-CM or ADSCs Increase Glioma C6 Cells Migration

Further, we evaluated the ability of ASCD-CM to affect tumor cell migration. First, the ability of ADSC-CM to affect glioma cell migration was tested by a scratch wound model in which C6 cells were treated with ADSC-CM-SF. Treatment of glioma C6 with CM24 or CM48 reveals a significant increase in
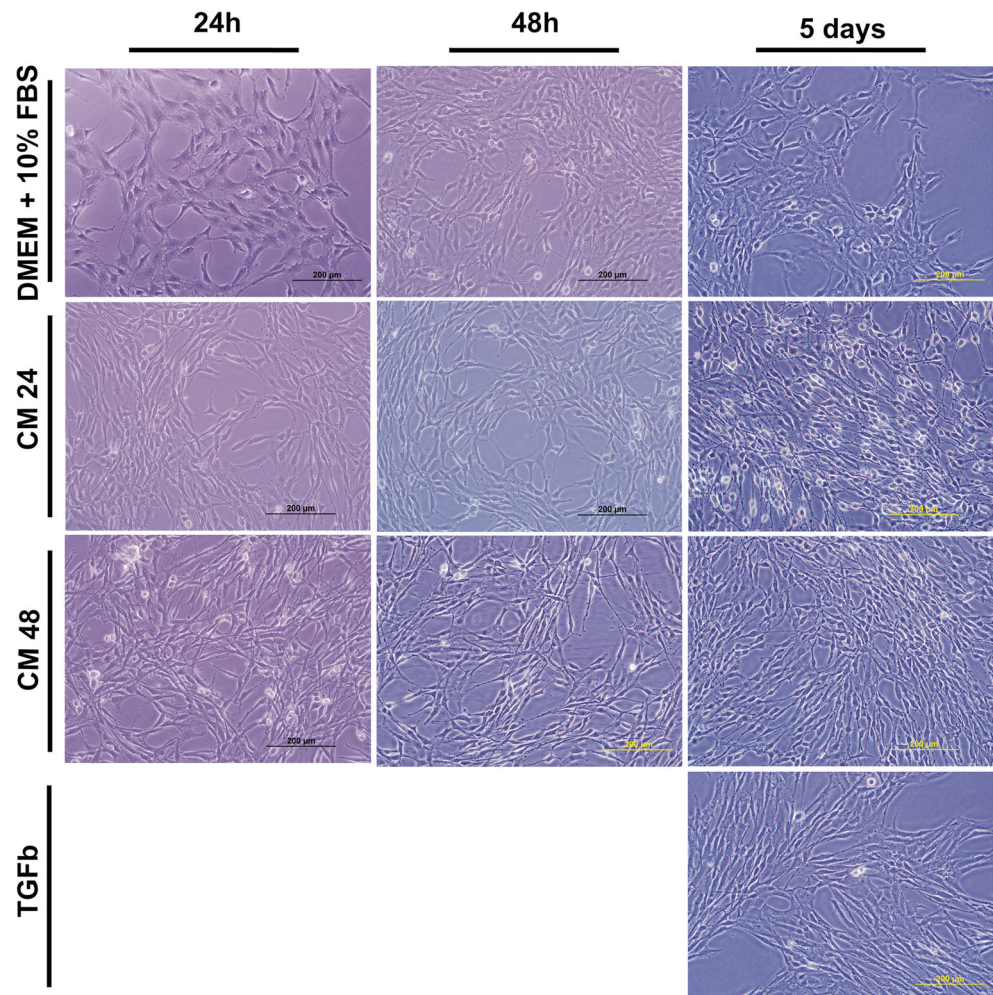
migration (2- and 1.7-fold, respectively) when compared with control (DMEM SF), an effect that became significant after 24 h (Fig. 2b, c).

Next, we tested in a Transwell system if the presence of ADSCs in the basal compartment could induce a stronger response than that generated by ADSC-CM. Glioma cells exhibited a 2.5-fold and 2-fold increase in cell migration when compared to negative control (DMEM SF), after 24 or 48 h of indirect co-culture of ADSCs and C6 cells, respectively (Fig. 2d, e).

Morphological Changes in C6 Glioma Cells Treated with ADSC-CM

Changes in the migratory profile of cells are tightly associated with alterations in cell spreading and cytoskeleton organization. When glioma cells were maintained in ADSC-CM, morphological changes in the majority of tumor cells could be observed. Cells treated with CM shifted from the epithelial-like cobblestone morphology to the spindle-like fibroblastoid appearance, when compared with untreated cells over the same period of time (Fig. 3).

Moreover, ADSC-CM induced characteristic reorganization of actin filaments after 24 h, 48 h, and 5 days of culture with CM, as detected by phalloidin-fluorescein labeling (Fig. 4). This result was observed mainly in CM48 treatment and on a smaller scale in CM24 treatment, but it was not observed in C6 cultured in control medium. ADSCs were observed to have F-actin filaments organized along the length of the cell as an elongated rod shape, reflecting a change in cellular polarity. Our results also showed that changes in cell morphology were accompanied by increased nuclear irregularity, mainly due to a circular to fusiform transition, suggesting that the EMT-like effect induced by CM is similar to TGFβ-induced EMT when nuclear morphology is considered, suggesting that TGFβ could be one of the factors present in CM that induces EMT-like process in C6 cells (Fig. 5).

ADSC-CM Enhance Expression of Markers Associated with EMT

Lastly, up-regulation of the EMT-associated markers in C6 cells exposed to ADSC-CM was confirmed. We analyzed
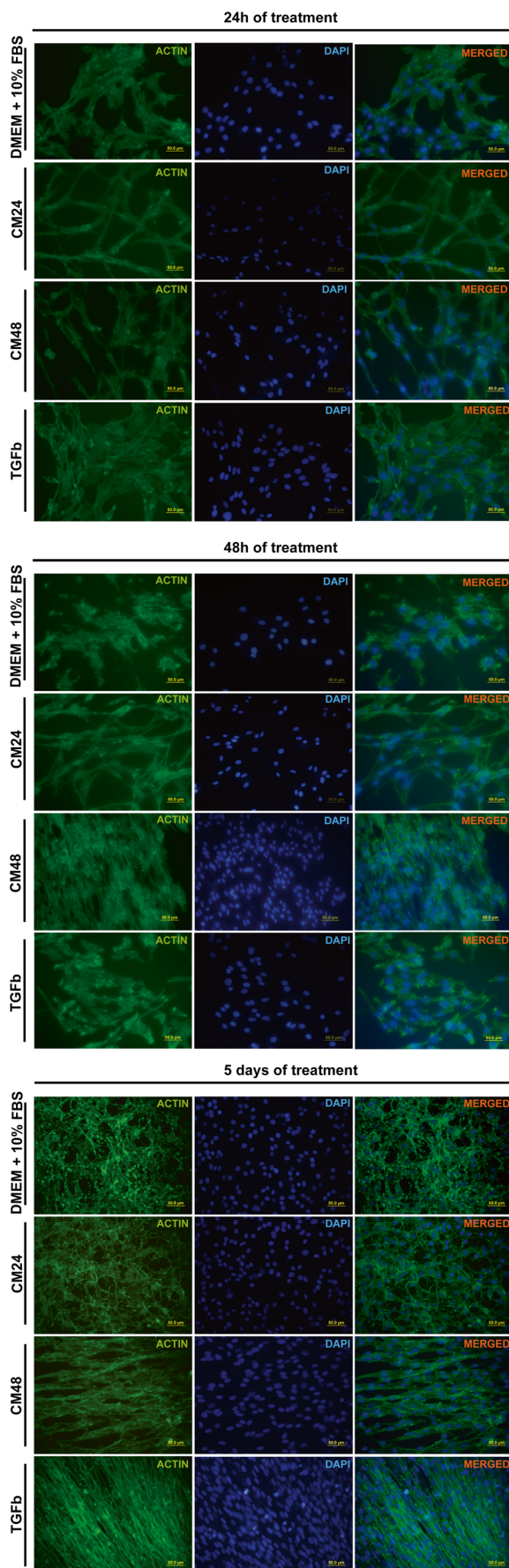

Fig. 3 Morphological appearance of C6 cells treated with ADSC-CM. Phase contrast microscopic views of C6 cells treated with ADSC-CM during 24 h, 48 h and 5 days. Positive control cells were treated for 5 days with 1 ng/mL TGF-β. *Scales bars*, 200 μm

◀ **Fig 4** F-actin fiber formation in C6 cells induced by ADSC-CM and TGF-β. Representative images of actin cytoskeleton reorganization via filamentous actin (F-actin) immunostained with DAPI and phalloidin-fluorescein. Cells were treated during 24 h, 48 h and 5 days with ADSC-CM. Negative and positive controls were performed by treatment with DMEM + 10 % FBS and 1 ng/mL TGF-β, respectively. All images presented are at ×400 magnification

the mRNA expression of vimentin, MMP2, NRAS, and Src mRNA and found that ADSC-CM48 was able to significantly increase the expression of vimentin and NRAS after 24 h of treatment, whereas after 48 h of cell exposure to CM, the expression of MMP2, vimentin and NRAS were upregulated. The expression of Src was not altered by ADSC-CM (Fig. 6). These data further support that treatment of C6 tumor cells with ADSC-CM promotes activation of signaling pathways leading to "reprogramming" of tumor cells toward a mesenchymal phenotype.

Discussion

Increasing evidence has shown that MSCs play a tumor-promoting function by stimulating tumor growth, invasion, motility, and anticancer-drug resistance mainly by interacting with cancer cells and promoting EMT [19, 32, 48–51]. Since MSCs are recruited to sites of growing tumor, there is a continuous and bilateral molecular crosstalk between stromal cells and cancer cells mediated through direct cell-cell contacts or by secreted molecules [52, 53]. Although it remains unclear whether physical contact between MSCs and tumor cells is really required [54], it seems almost certain that the major mechanism of MSC participation in cancer development is related to their paracrine activity [55]. Hence, the mechanisms of the modulatory behavior of MSCs must be explored and the use of MSCs in patients with cancer should be performed with caution.

Interestingly, we observed that ADSC-CM promotes a marked increase in cancer cell migration. Recent reports have shown a significant increase in migration of breast cancer cells [48, 56], gastric cancer cells [57], hepatic cells [58], esophageal carcinoma cells [59], and colon cancer cells [60] in response to factors secreted by MSCs. Increased migration is a key event to cellular invasiveness and is involved in degradation of basement membrane and extracellular matrix as well as vessel invasion. For occurrence of this process, it is necessary a paracrine communication through extracellular signals released by stromal tumor cells, synthesis of proteins, and active intracellular signaling with cytoskeleton proteins [34]. Several genes involved in glioma invasiveness have been identified and include members of the family of metalloproteases (MMP). Expression of MMP-2 and MMP-9 correlate with invasiveness, proliferation, and prognosis in astrocytomas [61].
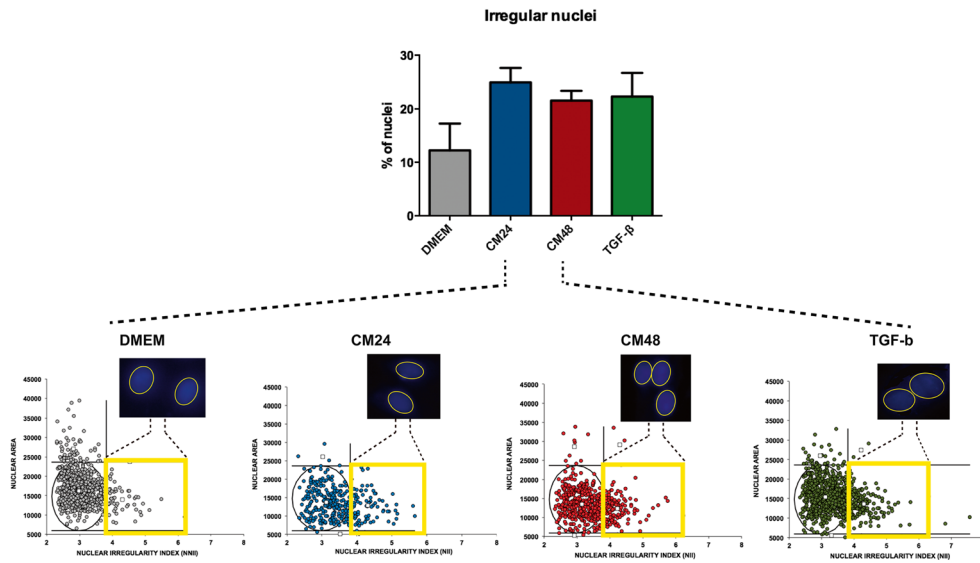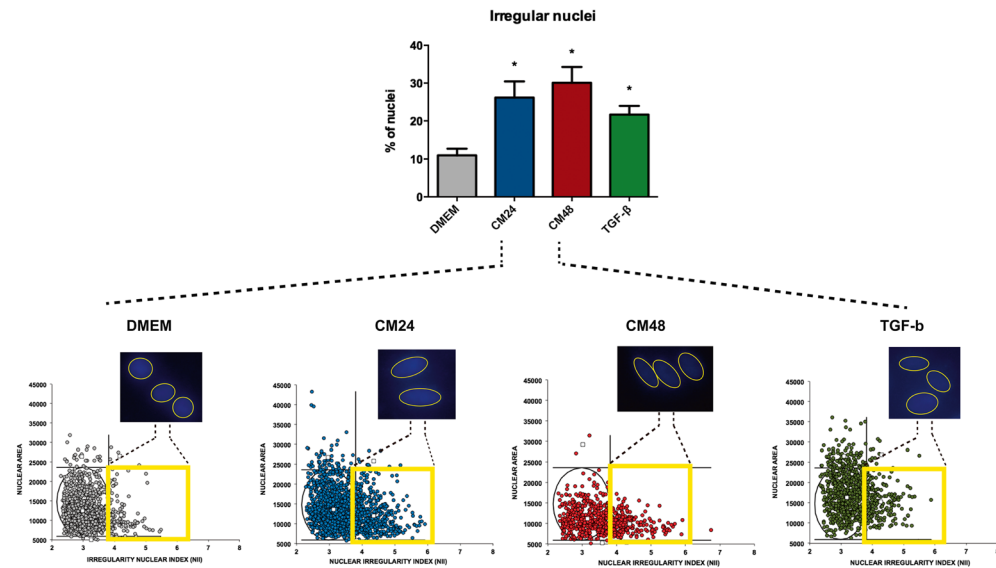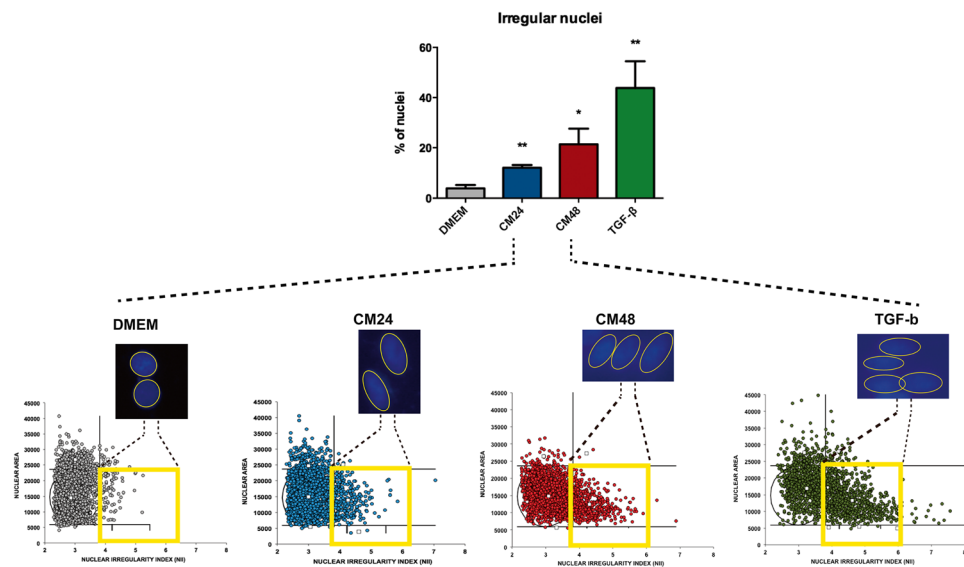
◄ **Fig 5** Morphologic nuclear changes in C6 cells treated with ADSC-CM. Distribution of C6 cells according to nuclear morphology. *Black circles* mark the normal nuclear morphology. Cells into the *yellow squares* represent cells with nuclear irregularity. Representative microphotographs (×40) showing the effect of CM in nuclear morphology of C6 cells. Results are expressed in percentage and were analyzed by one-way ANOVA, followed by Tukey's multiple comparisons test. The values were considered significantly different from controls, when $P < 0.05$. All experiments were repeated at least three times

Reinforcing this pro-spreading effect of MSCs in cancer cells, Karnoub et al. showed that bone marrow-derived human MSC when co-injected with breast carcinoma cells, in immunocompromised mice, are able to promote a marked enhancement in lung tumor metastasis, when compared to tumors composed only by cancer cells. Additionally, this effect on invasive potential was only observed when MSCs were injected close to the engraft tumor. These results demonstrate the importance of the tumor microenvironment and that cancer cells can respond in a transient way to signals received from their stromal microenvironment [62]. Although the metastasis of GBM already has been described in the literature [63], they remain very uncommon. The rapid relapse of tumor in GBM patients has been considered as the key factor of the lack of distant metastasis in patients with high-grade malignant gliomas [64]. However, despite metastasis outside of the CNS is not common in this type of tumor, the capacity to infiltrate and spread throughout the brain is a hallmark of GBM and is the main basis for the failure of treatment [65].

In our findings, the secretome of ADSCs was able to increase cell migration even without the physical presence of ADSCs. However, this effect was increased in the co-culture

Transwell system, in which cells share the same medium, but without direct contact. This can be explained by the fact that when different cells are together in the same microenvironment, the crosstalk among them is favored. In this case, the crosstalk could be favorable to cancer progression, once cancer cells could also release factors to modulate MSCs in its favor [24].

EMT is related to a more invasive cancer cell phenotype. This process is only possible because the detachment of tumor cells from the primary tumor is facilitated through the loss of cell-cell adhesion molecules [66]. Cells of epithelial origin are in part characterized by extensive points of cell-cell contact that maintain cells as a layer, whereas mesenchymal cells present only few contact points on their surface which mediate their interaction with neighboring cells, decreasing their adherence capacity [67]. In accordance, we demonstrate that C6 cells, after treatment with ADSC-CM, have their capacity of adhesion significantly reduced. This is compatible with EMT phenotype, in which cell adhesion molecules, such as cadherin, have their expression or function changed, promoting carcinoma progression and metastasis [68].

In order to confirm whether the decreased adhesion capacity and enhanced migration ability of C6 cells after CM treatment could be associated with EMT, we evaluate other hallmark features of EMT that are loss of apico-basal polarity, reorganization of cytoskeletal architecture, and changes in cell shape [69]. Epithelial cells are highly polarized apico-basally, which is manifested through the organization of the cytoskeleton. Mesenchymal cells show front-back polarity instead of apico-basal polarity [67]. Not surprisingly, we observed a marked demodulation of actin cytoskeleton, morphology changes, and characteristic elongated shape of the nucleus in
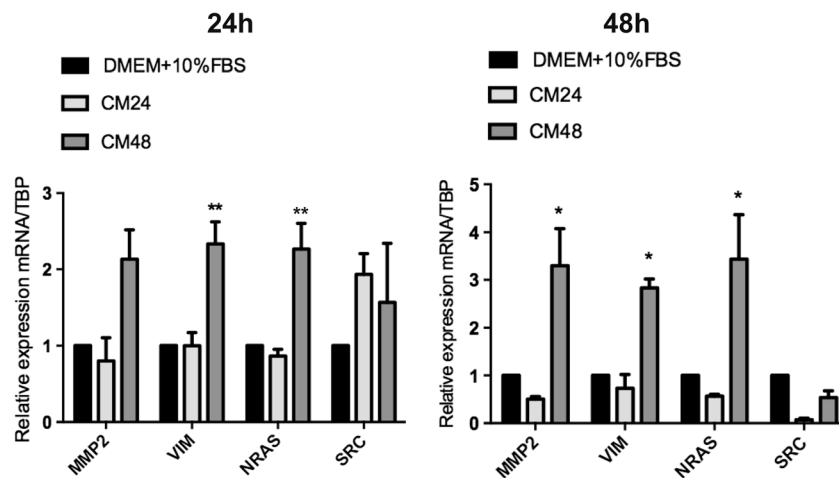

Fig 6 Expression of EMT Markers in the C6 glioma cells cultured in ADSC-CM. Quantitative RT-PCR confirmed significant increase in the mRNA expression of vimentin, MMP2, NRAS, and Src in C6 cells exposed during 24 and 48 h to ADSC-CM in comparison to C6 cells maintained under the standard culture conditions. Quantitative PCR measurements of gene expression levels are normalized against TBP levels, and expressed relatively to the control samples. The values were considered significantly different from controls, when $P < 0.05$ as determined by ANOVA followed by Tukey's test. *$p < 0.05$ and ***$p < 0.001$ indicate statistical difference from control. All experiments were repeated at least three times

CM-treated C6 cells. Therefore, we consider that the treatment with CM leads to an enhanced potential for cell motility, mainly due to cytoskeletal modulation in C6 cells.

Next, the genetic markers associated with EMT, vimentin, MMP2, NRAS, and Src were examined in C6 cancer cells following CM treatment. The results showed that with exception of the Src marker, the treatment with ADSC-CM 48 was capable to significantly increase the expression of EMT-associated genes. The matrix metalloproteinase MMP2 and the cytoskeletal protein vimentin are extensively described to be associated with increased migration after EMT [67]. Furthermore, the vimentin and MMP-2 up-regulation correlate with enhanced migration and invasion in many human

tumors, including glioblastoma [70–79]. Oncogenes have also been reported to be involved with EMT [80, 81]. In malignant human melanoma, NRAS/BRAF activation drives a switch in EMT transcription factor expression, leading to changes in favor of TWIST1 and ZEB1 [82]. In human pancreatic cancer cell line, Snail, a key regulator of EMT, can be induced by TGF-β in tumor cells and this induction is highly dependent on cooperation with active RAS signals [83]. Finally, the expression of Src was not altered by ADSC-CM in our study and probably the enhanced expression of this gene is not crucial to EMT induction. Additionally, tumor cells were shown to undergo an "incomplete" EMT. In other words, cells could progress through an intermediate epithelial/mesenchymal hybrid
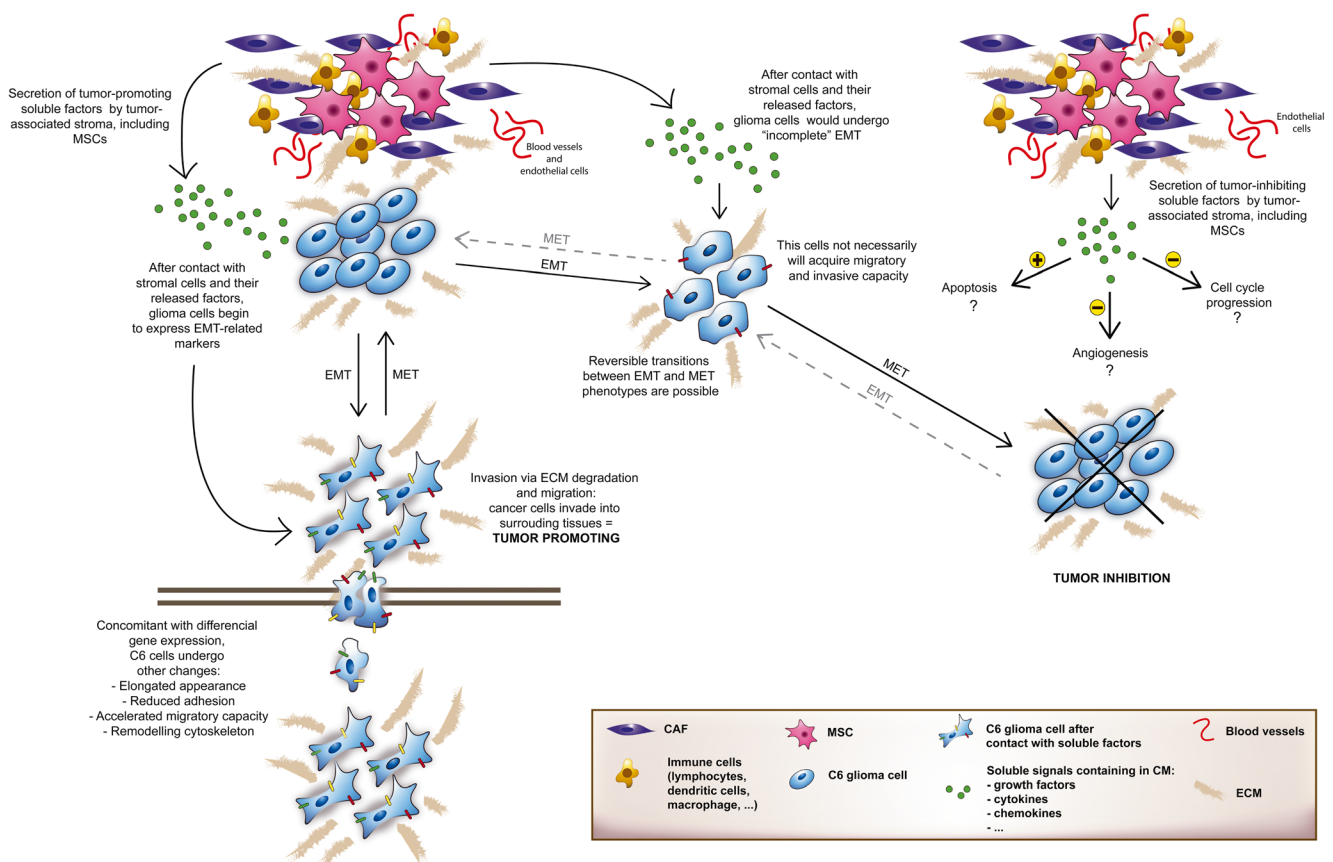

Fig 7 Schematic overview of the role of MSC-released factors in tumor progression. MSCs are known to be able to migrate and home to the tumor stroma. Within the tumor microenvironment, MSCs can deliver trophic factors, including growth factors, chemokines, and cytokines, which influence cancer cell phenotypes. MSC-derived factors can interact with receptors on C6 cell surface and activate signal transduction, resulting in loss of cell-cell contact and cobblestone appearance that lead to a more elongated cell shape, with front-back polarity. These cancer cells could show enhanced expression of EMT-related markers such as vimentin, MMP2, and NRAS. The crosstalk between MSCs and cancer cells also impact in subsequent stimulation of migratory capacity, leading to a spreading of tumor cells and cancer progression. On the other hand, factors released by MSCs can promote differences in cellular responses and trigger a partial or incomplete EMT in gliomas cells. Additionally, cancer cells can switch between epithelial

or mesenchymal phenotypes several times during formation of the complex crosstalk between tumor cells and its microenvironment. In this context, one has to keep in mind that EMT is a reversible process and the initiation of signal transduction cascades that drive EMT in epithelial cancer cells manifests in different levels in distinct cell types. Furthermore, when cells acquire an intermediate state of EMT, not necessarily will these cells be compromised with cancer progression, but in opposite, these cells can stay in a senescent state and be inhibited by the surrounding stroma or return through MET to an epithelial phenotype. At the end, if the stimulus of the tumor stroma surrounding was negative, an inhibitory effect into the tumor can limit tumor progression and result in disadvantage for tumor survival, without cells initiate the EMT changes. *EMT* epithelial to mesenchymal transition, *MET* mesenchymal to epithelial transition, *CAF* cancer-associated fibroblasts, *MSC* mesenchymal stem cell, *ECM* extracellular matrix

stage and acquire a metastatic and invasive phenotype without a requirement for a complete EMT as can be seen in Fig. 7 [84, 85]. In a model of murine mammary epithelial cell line, EpH4, the activation of MEK1 signaling can induce changes associated with EMT, such as enhanced motility, invasiveness, and remodeling of the actin cytoskeleton. However, no reduction in the levels of E-cadherin was observed, nor was there any induction of mesenchymal markers, such as smooth muscle actin or vimentin (Pinkas J). The incomplete EMT could be explained by the complexity of the EMT regulation network, most often resulting in a small subset of tumor cells advancing into the EMT program. Consequently, the induction of a full EMT in cancer cells is difficult to observe [86].

It is well-established that tumor cells work to stimulate their tumor-stromal cells to create a favorable environment for their survival [87]. Then, in accordance with the hypothesis that MSCs could support tumor progression, our analysis of cell cycle and cell viability showed that ADSC-CM is unable to alter C6 viability or the progression in cell cycle, thereby allowing cell survival. The growth rate of C6 cells in our model was not changed after CM cell treatment. Until now, there is no consensus in the literature about the effect of MSCs on cancer cells proliferation, with some studies reporting inhibition [7, 28, 48], stimulation [26, 28], or no change [88]. Therefore, we consider that these conflicting findings are due differences in cell source, model of cancer tested, or species studied. There is scant information in the scientific literature regarding the association between stem cells and EMT in gliomas. One of the few works found showed that CD133+ glioma stem cell treated with human umbilical cord blood derived-MSCs presented a down regulation of Twist1 and Sox2 proteins, losing their stemness feature, by reverting EMT through induction of mesenchymal epithelial transition (MET) [89]. This study reinforces the importance to take into account the origin and type of MSC before their therapeutic application.

In summary, in the current work, we explored the interaction between ADSCs and C6 glioma cell line through ADSC-CM to understand the effects of ADSC-secretome in tumor development. This report provides evidences that molecules secreted by rat ADSCs can mediate the induction of EMT-like transformation in C6 cancer cells. Despite the recognition of the role of EMT in the cancer progression, the mechanisms explaining how stimuli-induced EMT occurs at the tumor site remains unknown. Further understanding of the complex crosstalk between MSCs and tumor cells as well as the role that paracrine communication plays in tumor progression is required to establish the effectiveness and safety of treatment strategies using cell therapy in gliomas. An overview to a better comprehension about the intricate communication between cancer cells and their microenvironment is provided in Fig. 7.

Compliance with Ethical Standards

Competing Interests The authors declare that they have no competing interests.

References

1. Becker KP, Yu J (2012) Status quo—standard-of-care medical and radiation therapy for glioblastoma. Cancer J 18(1):12–19. doi:10.1097/PPO.0b013e318244d7eb

2. Lima FR, Kahn SA, Soletti RC, Biasoli D, Alves T, da Fonseca AC, Garcia C, Romao L et al (2012) Glioblastoma: therapeutic challenges, what lies ahead. Biochim Biophys Acta 1826(2):338–349. doi:10.1016/j.bbcan.2012.05.004

3. Westphal M, Lamszus K (2011) The neurobiology of gliomas: from cell biology to the development of therapeutic approaches. Nat Rev Neurosci 12(9):495–508. doi:10.1038/nrn3060

4. Holland EC (2000) Glioblastoma multiforme: the terminator. Proc Natl Acad Sci U S A 97(12):6242–6244

5. Catalano V, Turdo A, Di Franco S, Dieli F, Todaro M, Stassi G (2013) Tumor and its microenvironment: a synergistic interplay. Semin Cancer Biol 23(6 Pt B):522–532. doi:10.1016/j.semcancer.2013.08.007

6. Dvorak HF (1986) Tumors: wounds that do not heal. Similarities between tumor stroma generation and wound healing. N Engl J Med 315(26):1650–1659. doi:10.1056/NEJM198612253152606

7. Martin FT, Dwyer RM, Kelly J, Khan S, Murphy JM, Curran C, Miller N, Hennessy E et al (2010) Potential role of mesenchymal stem cells (MSCs) in the breast tumour microenvironment: stimulation of epithelial to mesenchymal transition (EMT). Breast Cancer Res Treat 124(2):317–326. doi:10.1007/s10549-010-0734-1

8. Chagastelles PC, Nardi NB, Camassola M (2010) Biology and applications of mesenchymal stem cells. Sci Prog 93(Pt 2):113–127

9. Meirelles Lda S, Fontes AM, Covas DT, Caplan AI (2009) Mechanisms involved in the therapeutic properties of mesenchymal stem cells. Cytokine Growth Factor Rev 20(5–6):419–427. doi:10.1016/j.cytogfr.2009.10.002

10. Glaser T, Cappellari AR, Pillat MM, Iser IC, Wink MR, Battastini AM, Ulrich H (2012) Perspectives of purinergic signaling in stem cell differentiation and tissue regeneration. Purinergic Signal 8(3):523–537. doi:10.1007/s11302-011-9282-3

11. Iser IC, Bracco PA, Goncalves CE, Zanin RF, Nardi NB, Lenz G, Battastini AM, Wink MR (2014) Mesenchymal stem cells from different murine tissues have differential capacity to metabolize extracellular nucleotides. J Cell Biochem 115(10):1673–1682. doi:10.1002/jcb.24830

12. Altaner C, Altanerova V (2012) Stem cell based glioblastoma gene therapy. Neoplasma 59(6):756–760. doi:10.4149/neo_2012_95

13. Nakamizo A, Marini F, Amano T, Khan A, Studeny M, Gumin J, Chen J, Hentschel S et al (2005) Human bone marrow-derived mesenchymal stem cells in the treatment of gliomas. Cancer Res 65(8):3307–3318. doi:10.1158/0008-5472.CAN-04-1874

14. Kucerova L, Altanerova V, Matuskova M, Tyciakova S, Altaner C (2007) Adipose tissue-derived human mesenchymal stem cells mediated prodrug cancer gene therapy. Cancer Res 67(13):6304–6313. doi:10.1158/0008-5472.CAN-06-4024

15. Bak XY, Lam DH, Yang J, Ye K, Wei EL, Lim SK, Wang S (2011) Human embryonic stem cell-derived mesenchymal stem cells as cellular delivery vehicles for prodrug gene therapy of glioblastoma. Hum Gene Ther 22(11):1365–1377. doi:10.1089/hum.2010.212

16. Chien LY, Hsiao JK, Hsu SC, Yao M, Lu CW, Liu HM, Chen YC, Yang CS, Huang DM In vivo magnetic resonance imaging of cell tropism, trafficking mechanism, and therapeutic impact of human mesenchymal stem cells in a murine glioma model. Biomaterials 32(12):3275–3284. doi: 10.1016/j.biomaterials.2011.01.042

17. Bianchi G, Morandi F, Cilli M, Daga A, Bocelli-Tyndall C, Gambini C, Pistoia V, Raffaghello L (2012) Close interactions between mesenchymal stem cells and neuroblastoma cell lines lead to tumor growth inhibition. PLoS ONE 7(10):e48654. doi:10.1371/journal.pone.0048654

18. Beckermann BM, Kallifatidis G, Groth A, Frommhold D, Apel A, Mattern J, Salnikov AV, Moldenhauer G et al (2008) VEGF expression by mesenchymal stem cells contributes to angiogenesis in pancreatic carcinoma. Br J Cancer 99(4):622–631. doi:10.1038/sj.bjc.6604508

19. De Luca A, Lamura L, Gallo M, Maffia V, Normanno N Mesenchymal stem cell-derived interleukin-6 and vascular endothelial growth factor promote breast cancer cell migration. J Cell Biochem 113 (11):3363–3370. doi:10.1002/jcb.24212

20. Kang SG, Jeun SS, Lim JY, Kim SM, Yang YS, Oh WI, Huh PW, Park CK (2008) Cytotoxicity of human umbilical cord blood-derived mesenchymal stem cells against human malignant glioma cells. Childs Nerv Syst ChNS Off J Int Soc Pediatr Neurosurg 24(3):293–302. doi:10.1007/s00381-007-0515-2

21. Chien LY, Hsiao JK, Hsu SC, Yao M, Lu CW, Liu HM, Chen YC, Yang CS et al (2011) In vivo magnetic resonance imaging of cell tropism, trafficking mechanism, and therapeutic impact of human mesenchymal stem cells in a murine glioma model. Biomaterials 32(12):3275–3284. doi:10.1016/j.biomaterials.2011.01.042

22. Jiao H, Guan F, Yang B, Li J, Shan H, Song L, Hu X, Du Y (2011) Human umbilical cord blood-derived mesenchymal stem cells inhibit C6 glioma via downregulation of cyclin D1. Neurol India 59(2):241–247. doi:10.4103/0028-3886.79134

23. Pisati F, Belicchi M, Acerbi F, Marchesi C, Giussani C, Gavina M, Javerzat S, Hagedorn M et al (2007) Effect of human skin-derived stem cells on vessel architecture, tumor growth, and tumor invasion in brain tumor animal models. Cancer Res 67(7):3054–3063. doi:10.1158/0008-5472.CAN-06-1384

24. Liu J, Zhang Y, Bai L, Cui X, Zhu J (2012) Rat bone marrow mesenchymal stem cells undergo malignant transformation via indirect co-cultured with tumour cells. Cell Biochem Funct 30(8):650–656. doi:10.1002/cbf.2844

25. Yu JM, Jun ES, Bae YC, Jung JS (2008) Mesenchymal stem cells derived from human adipose tissues favor tumor cell growth in vivo. Stem Cells Dev 17(3):463–473. doi:10.1089/scd.2007.0181

26. Behnan J, Isakson P, Joel M, Cilio C, Langmoen IA, Vik-Mo EO, Badn W (2014) Recruited brain tumor-derived mesenchymal stem cells contribute to brain tumor progression. Stem Cells 32(5):1110–1123. doi:10.1002/stem.1614

27. Ochs K, Sahm F, Opitz CA, Lanz TV, Oezen I, Couraud PO, von Deimling A, Wick W et al (2013) Immature mesenchymal stem cell-like pericytes as mediators of immunosuppression in human malignant glioma. J Neuroimmunol 265(1–2):106–116. doi:10.1016/j.jneuroim.2013.09.011

28. Akimoto K, Kimura K, Nagano M, Takano S, To'a Salazar G, Yamashita T, Ohneda O (2013) Umbilical cord blood-derived mesenchymal stem cells inhibit, but adipose tissue-derived mesenchymal stem cells promote, glioblastoma multiforme proliferation. Stem Cells Dev 22(9):1370–1386. doi:10.1089/scd.2012.0486

29. Barcellos-de-Souza P, Gori V, Bambi F, Chiarugi P (2013) Tumor microenvironment: bone marrow-mesenchymal stem cells as key players. Biochim Biophys Acta 1836(2):321–335. doi:10.1016/j.bbcan.2013.10.004

30. Kahlert UD, Nikkhah G, Maciaczyk J (2013) Epithelial-to-mesenchymal(-like) transition as a relevant molecular event in malignant gliomas. Cancer Lett 331(2):131–138. doi:10.1016/j.canlet.2012.12.010

31. Kalluri R, Weinberg RA (2009) The basics of epithelial-mesenchymal transition. J Clin Invest 119(6):1420–1428. doi:10.1172/JCI39104

32. Kabashima-Niibe A, Higuchi H, Takaishi H, Masugi Y, Matsuzaki Y, Mabuchi Y, Funakoshi S, Adachi M et al (2013) Mesenchymal stem cells regulate epithelial-mesenchymal transition and tumor progression of pancreatic cancer cells. Cancer Sci 104(2):157–164. doi:10.1111/cas.12059

33. Jung Y, Kim JK, Shiozawa Y, Wang J, Mishra A, Joseph J, Berry JE, McGee S et al (2013) Recruitment of mesenchymal stem cells into prostate tumours promotes metastasis. Nat Commun 4:1795. doi:10.1038/ncomms2766

34. Jing Y, Han Z, Liu Y, Sun K, Zhang S, Jiang G, Li R, Gao L et al (2012) Mesenchymal stem cells in inflammation microenvironment accelerates hepatocellular carcinoma metastasis by inducing epithelial-mesenchymal transition. PLoS ONE 7(8):e43272. doi:10.1371/journal.pone.0043272

35. Xu Q, Wang L, Li H, Han Q, Li J, Qu X, Huang S, Zhao RC (2012) Mesenchymal stem cells play a potential role in regulating the establishment and maintenance of epithelial-mesenchymal transition in MCF7 human breast cancer cells by paracrine and induced autocrine TGF-beta. Int J Oncol 41(3):959–968. doi:10.3892/ijo.2012.1541

36. da Silva Meirelles L, Chagastelles PC, Nardi NB (2006) Mesenchymal stem cells reside in virtually all post-natal organs and tissues. J Cell Sci 119(Pt 11):2204–2213

37. Overton WR, McCoy JP Jr (1994) Reversing the effect of formalin on the binding of propidium iodide to DNA. Cytometry 16(4):351–356. doi:10.1002/cyto.990160410

38. Wang L, Zhou X, Zhou T, Ma D, Chen S, Zhi X, Yin L, Shao Z et al (2008) Ecto-5'-nucleotidase promotes invasion, migration and adhesion of human breast cancer cells. J Cancer Res Clin Oncol 134(3):365–372. doi:10.1007/s00432-007-0292-z

39. Liang CC, Park AY, Guan JL (2007) In vitro scratch assay: a convenient and inexpensive method for analysis of cell migration in vitro. Nat Protoc 2(2):329–333. doi:10.1038/nprot.2007.30

40. Zhang D, LaFortune TA, Krishnamurthy S, Esteva FJ, Cristofanilli M, Liu P, Lucci A, Singh B et al (2009) Epidermal growth factor receptor tyrosine kinase inhibitor reverses mesenchymal to epithelial phenotype and inhibits metastasis in inflammatory breast cancer. Clin Cancer Res Off J Am Assoc Cancer Res 15(21):6639–6648. doi:10.1158/1078-0432.CCR-09-0951

41. Zhan R, Yang S, He W, Wang F, Tan J, Zhou J, Yang S, Yao Z et al (2015) Nitric oxide enhances keratinocyte cell migration by regulating Rho GTPase via cGMP-PKG signalling. PLoS ONE 10(3):e0121551. doi:10.1371/journal.pone.0121551

42. Filippi-Chiela EC, Oliveira MM, Jurkovski B, Callegari-Jacques SM, da Silva VD, Lenz G (2012) Nuclear morphometric analysis (NMA): screening of senescence, apoptosis and nuclear irregularities. PLoS ONE 7(8):e42522. doi:10.1371/journal.pone.0042522

43. Iser IC CR, Bertoni APS, Wink MR (2015) Identification of valid endogenous control genes for determining gene expression in C6 glioma cell line treated with conditioned medium from adipose-

derived stem cell. Biomed Pharmacother 75:75–82. doi:10.1016/j.biopha.2015.08.035

44. Livak KJ, Schmittgen TD (2001) Analysis of relative gene expression data using real-time quantitative PCR and the 2(-Delta Delta C(T)) method. Methods 25(4):402–408. doi:10.1006/meth.2001.1262

45. Gutierrez-Fernandez M, Rodriguez-Frutos B, Ramos-Cejudo J, Teresa Vallejo-Cremades M, Fuentes B, Cerdan S, Diez-Tejedor E (2013) Effects of intravenous administration of allogenic bone marrow- and adipose tissue-derived mesenchymal stem cells on functional recovery and brain repair markers in experimental ischemic stroke. Stem Cell Res Ther 4(1):11. doi:10.1186/scrt159

46. Shirkoohi R (2013) Epithelial mesenchymal transition from a natural gestational orchestration to a bizarre cancer disturbance. Cancer Sci 104(1):28–35. doi:10.1111/cas.12074

47. Sanchez-Tillo E, Liu Y, de Barrios O, Siles L, Fanlo L, Cuatrecasas M, Darling DS, Dean DC et al (2012) EMT-activating transcription factors in cancer: beyond EMT and tumor invasiveness. Cell Mol Life Sci CMLS 69(20):3429–3456. doi:10.1007/s00018-012-1122-2

48. Kucerova L, Skolekova S, Matuskova M, Bohac M, Kozovska Z (2013) Altered features and increased chemosensitivity of human breast cancer cells mediated by adipose tissue-derived mesenchymal stromal cells. BMC Cancer 13:535. doi:10.1186/1471-2407-13-535

49. Barbero S, Bonavia R, Bajetto A, Porcile C, Pirani P, Ravetti JL, Zona GL, Spaziante R et al (2003) Stromal cell-derived factor 1alpha stimulates human glioblastoma cell growth through the activation of both extracellular signal-regulated kinases 1/2 and Akt. Cancer Res 63(8):1969–1974

50. Prantl L, Muehlberg F, Navone NM, Song YH, Vykoukal J, Logothetis CJ, Alt EU (2010) Adipose tissue-derived stem cells promote prostate tumor growth. Prostate 70(15):1709–1715. doi:10.1002/pros.21206

51. Bhattacharya SD, Mi Z, Talbot LJ, Guo H, Kuo PC (2012) Human mesenchymal stem cell and epithelial hepatic carcinoma cell lines in admixture: concurrent stimulation of cancer-associated fibroblasts and epithelial-to-mesenchymal transition markers. Surgery 152(3):449–454. doi:10.1016/j.surg.2012.06.011

52. Hong IS, Lee HY, Kang KS (2014) Mesenchymal stem cells and cancer: friends or enemies? Mutat Res 768:98–106. doi:10.1016/j.mrfmmm.2014.01.006

53. Zimmerlin L, Park TS, Zambidis ET, Donnenberg VS, Donnenberg AD (2013) Mesenchymal stem cell secretome and regenerative therapy after cancer. Biochimie 95(12):2235–2245. doi:10.1016/j.biochi.2013.05.010

54. Zhu W, Huang L, Li Y, Qian H, Shan X, Yan Y, Mao F, Wu X et al (2011) Mesenchymal stem cell-secreted soluble signaling molecules potentiate tumor growth. Cell Cycle 10(18):3198–3207

55. Makridakis M, Roubelakis MG, Vlahou A (2013) Stem cells: insights into the secretome. Biochim Biophys Acta 1834(11):2380–2384. doi:10.1016/j.bbapap.2013.01.032

56. Corcoran KE, Trzaska KA, Fernandes H, Bryan M, Taborga M, Srinivas V, Packman K, Patel PS et al (2008) Mesenchymal stem cells in early entry of breast cancer into bone marrow. PLoS ONE 3(6):e2563. doi:10.1371/journal.pone.0002563

57. Xue Z, Wu X, Chen X, Liu Y, Wang X, Wu K, Nie Y, Fan D (2015) Mesenchymal stem cells promote epithelial to mesenchymal transition and metastasis in gastric cancer though paracrine cues and close physical contact. J Cell Biochem 116(4):618–627. doi:10.1002/jcb.25013

58. Li X, Luo Q, Sun J, Song G (2015) Conditioned medium from mesenchymal stem cells enhances the migration of hepatoma cells through CXCR4 up-regulation and F-actin remodeling. Biotechnol Lett 37(3):511–521. doi:10.1007/s10529-014-1710-3

59. Yang X, Li Z, Ma Y, Gao J, Liu S, Gao Y, Wang G (2014) Human umbilical cord mesenchymal stem cells promote carcinoma growth and lymph node metastasis when co-injected with esophageal carcinoma cells in nude mice. Cancer Cell Int 14(1):93. doi:10.1186/s12935-014-0093-9

60. Shinagawa K, Kitadai Y, Tanaka M, Sumida T, Kodama M, Higashi Y, Tanaka S, Yasui W et al (2010) Mesenchymal stem cells enhance growth and metastasis of colon cancer. Int J Cancer 127(10):2323–2333. doi:10.1002/ijc.25440

61. Wang M, Wang T, Liu S, Yoshida D, Teramoto A (2003) The expression of matrix metalloproteinase-2 and -9 in human gliomas of different pathological grades. Brain Tumor Pathol 20(2):65–72

62. Karnoub AE, Dash AB, Vo AP, Sullivan A, Brooks MW, Bell GW, Richardson AL, Polyak K et al (2007) Mesenchymal stem cells within tumour stroma promote breast cancer metastasis. Nature 449(7162):557–563. doi:10.1038/nature06188

63. Fonkem E, Lun M, Wong ET (2011) Rare phenomenon of extracranial metastasis of glioblastoma. J Clin Oncol Off J Am Soc Clin Oncol 29(34):4594–4595. doi:10.1200/JCO.2011.39.0187

64. Lombard A, Goffart N, Rogister B (2015) Glioblastoma circulating cells: reality, trap or illusion? Stem Cells Int 2015:182985. doi:10.1155/2015/182985

65. Furnari FB, Fenton T, Bachoo RM, Mukasa A, Stommel JM, Stegh A, Hahn WC, Ligon KL et al (2007) Malignant astrocytic glioma: genetics, biology, and paths to treatment. Genes Dev 21(21):2683–2710. doi:10.1101/gad.1596707

66. Jiang WG, Sanders AJ, Katoh M, Ungefroren H, Gieseler F, Prince M, Thompson SK, Zollo M et al (2015) Tissue invasion and metastasis: molecular, biological and clinical perspectives. Semin Cancer Biol. doi:10.1016/j.semcancer.2015.03.008

67. Kokkinos MI, Wafai R, Wong MK, Newgreen DF, Thompson EW, Waltham M (2007) Vimentin and epithelial-mesenchymal transition in human breast cancer—observations in vitro and in vivo. Cells Tissues Organs 185(1–3):191–203. doi:10.1159/000101320

68. Cavallaro U, Christofori G (2001) Cell adhesion in tumor invasion and metastasis: loss of the glue is not enough. Biochim Biophys Acta 1552(1):39–45

69. Lamouille S, Subramanyam D, Blelloch R, Derynck R (2013) Regulation of epithelial-mesenchymal and mesenchymal-epithelial transitions by microRNAs. Curr Opin Cell Biol 25(2):200–207. doi:10.1016/j.ceb.2013.01.008

70. Zhang Q, Helfand BT, Jang TL, Zhu LJ, Chen L, Yang XJ, Kozlowski J, Smith N et al (2009) Nuclear factor-kappaB-mediated transforming growth factor-beta-induced expression of vimentin is an independent predictor of biochemical recurrence after radical prostatectomy. Clin Cancer Res Off J Am Assoc Cancer Res 15(10):3557–3567. doi:10.1158/1078-0432.CCR-08-1656

71. McInroy L, Maatta A (2007) Down-regulation of vimentin expression inhibits carcinoma cell migration and adhesion. Biochem Biophys Res Commun 360(1):109–114. doi:10.1016/j.bbrc.2007.06.036

72. Hendrix MJ, Seftor EA, Chu YW, Seftor RE, Nagle RB, McDaniel KM, Leong SP, Yohem KH et al (1992) Coexpression of vimentin and keratins by human melanoma tumor cells: correlation with invasive and metastatic potential. J Natl Cancer Inst 84(3):165–174

73. Kidd ME, Shumaker DK, Ridge KM (2014) The role of vimentin intermediate filaments in the progression of lung cancer. Am J Respir Cell Mol Biol 50(1):1–6. doi:10.1165/rcmb.2013-0314TR

74. Toiyama Y, Yasuda H, Saigusa S, Tanaka K, Inoue Y, Goel A, Kusunoki M (2013) Increased expression of slug and vimentin as novel predictive biomarkers for lymph node metastasis and poor prognosis in colorectal cancer. Carcinogenesis 34(11):2548–2557. doi:10.1093/carcin/bgt282

75. Hamasaki T, Hattori T, Kimura G, Nakazawa N (1998) Tumor progression and expression of matrix metalloproteinase-2 (MMP-

2) mRNA by human urinary bladder cancer cells. Urol Res 26(6): 371–376

76. Hofmann UB, Westphal JR, Waas ET, Zendman AJ, Cornelissen IM, Ruiter DJ, van Muijen GN (1999) Matrix metalloproteinases in human melanoma cell lines and xenografts: increased expression of activated matrix metalloproteinase-2 (MMP-2) correlates with melanoma progression. Br J Cancer 81(5):774–782. doi:10.1038/sj.bjc.6690763

77. Trudel D, Fradet Y, Meyer F, Harel F, Tetu B (2003) Significance of MMP-2 expression in prostate cancer: an immunohistochemical study. Cancer Res 63(23):8511–8515

78. Durlik M, Gardian K (2012) Metalloproteinase 2 and 9 activity in the development of pancreatic cancer. Pol Przegl Chir 84(8):377–382. doi:10.2478/v10035-012-0064-6

79. Chintala SK, Tonn JC, Rao JS (1999) Matrix metalloproteinases and their biological function in human gliomas. Int J Dev Neurosci Off J Int Soc Dev Neurosci 17(5–6):495–502

80. Knobbe CB, Reifenberger J, Reifenberger G (2004) Mutation analysis of the Ras pathway genes NRAS, HRAS, KRAS and BRAF in glioblastomas. Acta Neuropathol 108(6):467–470. doi:10.1007/s00401-004-0929-9

81. Bleeker FE, Lamba S, Rodolfo M, Scarpa A, Leenstra S, Vandertop WP, Bardelli A (2009) Mutational profiling of cancer candidate genes in glioblastoma, melanoma and pancreatic carcinoma reveals a snapshot of their genomic landscapes. Hum Mutat 30(2):E451–E459. doi:10.1002/humu.20927

82. Caramel J, Papadogeorgakis E, Hill L, Browne GJ, Richard G, Wierinckx A, Saldanha G, Osborne J et al (2013) A switch in the expression of embryonic EMT-inducers drives the development of malignant melanoma. Cancer Cell 24(4):466–480. doi:10.1016/j.ccr.2013.08.018

83. Horiguchi K, Shirakihara T, Nakano A, Imamura T, Miyazono K, Saitoh M (2009) Role of Ras signaling in the induction of snail by transforming growth factor-beta. J Biol Chem 284(1):245–253. doi:10.1074/jbc.M804777200

84. Christiansen JJ, Rajasekaran AK (2006) Reassessing epithelial to mesenchymal transition as a prerequisite for carcinoma invasion and metastasis. Cancer Res 66(17):8319–8326. doi:10.1158/0008-5472.CAN-06-0410

85. Strauss R, Hamerlik P, Lieber A, Bartek J (2012) Regulation of stem cell plasticity: mechanisms and relevance to tissue biology and cancer. Mol Ther J Am Soc Gene Ther 20(5):887–897. doi:10.1038/mt.2012.2

86. Scheel C, Onder T, Karnoub A, Weinberg RA (2007) Adaptation versus selection: the origins of metastatic behavior. Cancer Res 67(24):11476–11479. doi:10.1158/0008-5472.CAN-07-1653, discussion 11479–11480

87. Quail DF, Joyce JA (2013) Microenvironmental regulation of tumor progression and metastasis. Nat Med 19(11):1423–1437. doi:10.1038/nm.3394

88. Hombauer H, Minguell JJ (2000) Selective interactions between epithelial tumour cells and bone marrow mesenchymal stem cells. Br J Cancer 82(7):1290–1296. doi:10.1054/bjoc.1999.1093

89. Velpula KK, Dasari VR, Tsung AJ, Dinh DH, Rao JS (2011) Cord blood stem cells revert glioma stem cell EMT by down regulating transcriptional activation of Sox2 and Twist1. Oncotarget 2(12):1028–1042